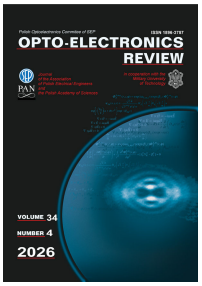
Opto-Electronics Review

journal homepage: publishinghouse.pan.pl/index.php/opelre



A study on the feasibility of culturing HMC3 cells using graphene and graphene oxide

Julia Radosz[1], Barbara Nasiłowska[2*], Marta Kutwin[3], Kamila Narojczyk[4], Dominik Pośląda[1], Paula Bień[4], Karolina Wiśniewska[3], Przemysław Zagrajek[2], Norbert Pałka[2], Zdzisław Bogdanowicz[5]

[1] Biophotonics Student Research Group, Institute of Optoelectronics, Military University of Technology, ul. gen. Sylwestra Kaliskiego 2, 00-908 Warsaw, Poland
[2] Institute of Optoelectronics, Military University of Technology, ul. gen. Sylwestra Kaliskiego 2, 00-908 Warsaw, Poland,
[3] Department of Nanobiotechnology, Institute of Biology, Warsaw University of Life Sciences, ul. Jana Ciszewskiego 8, 02-786 Warsaw, Poland
[4] Doctoral School, Military University of Technology, ul. gen. Sylwestra Kaliskiego 2, 00-908 Warsaw, Poland
[5] Faculty of Mechanical Engineering, Military University of Technology, ul. gen. Sylwestra Kaliskiego 2, 00-908 Warsaw, Poland

Article info

Article history:
Received 24 May 2026
Received in revised form 03 Oct. 2026
Accepted 03 Oct. 2026
Available online 13 Nov. 2026

Keywords:
graphene;
graphene oxide;
HMC3 cells.

Abstract

This publication presents the effects of graphene (G) and graphene oxide (GO) nanostructures on the morphology and viability of HMC3 microglial cells. Structural analyses were performed on G and GO layers deposited on a polished silicon wafer, including scanning electron microscopy (SEM) and Fourier-transform infrared spectroscopy (FTIR), as well as terahertz (THz) spectroscopy. The publication primary objective was to investigate the interaction between selected G and GO nanostructure substrates and HMC3 cells. Studies showed that the viability of HMC3 cells cultured on GO increased, respectively, possibly due to changes in surface morphology. These results may lay the groundwork for new regenerative medicine therapies and cell culture platforms.

1. Introduction

More than 100 000 patients undergo neurosurgical procedures in the United States and Europe each year [1, 2]. However, nerve regeneration remains the greatest challenge for modern neurosurgery, and the number of nerve injuries caused by degenerative diseases and trauma continues to rise.

Nerve cells are the primary structural units of the nervous system and play a significant role in maintaining the body balance by controlling the activity of all organs [3]. The two main classes of cells present in the nervous system are neurons, which can conduct and generate electrical impulses, and glia, which are considered non-excitable [4]. However, both have a limited ability to regenerate following injury or disease, which can lead to sensory or motor disorders and significantly reduce patients' quality of life and ability to function. The absence of Schwann cells in their structure prevents axon growth and the presence of a glial scar creates unfavourable conditions for nerve regeneration. These structures are also difficult to culture in vitro, which poses a challenge when studying their behaviour and regeneration. To supplement the current literature, this study investigated the potential use of graphene nanostructure substrates to enable cell growth and proliferation [3].

Graphene (G) and graphene oxide (GO) are of interest due to their potential biomedical applications, primarily because of their unique properties, such as hydrophilicity, and their ability to interact with cells [5].

Compared to other nanomaterials, G also exhibits reduced cytotoxicity [6, 7]. G has found wide application in tissue engineering due to its ability to conduct electricity and absorb proteins and other small chemical molecules [8]. Its effect on adhesion varies depending on the state of the cells seeded on it beforehand. As a result of GO action, the cells adenosine triphosphate (ATP) levels decrease, leading to energy depletion and increased autophagy. This process eliminates non-adherent cells, which is particularly important in the case of cancer cells that are responsible for metastasis. The oxygen-containing functional groups of GO

*Corresponding author at: barbara.nasilowska@wat.edu.pl

https://doi.org/10.24425/opelre.2026.7672
1896-3757/ Association of Polish Electrical Engineers (SEP) and Polish Academy of Sciences (PAS). Published by PAS
© 2026 The Author(s). This is an open access article under the CC BY license (https://creativecommons.org/licenses/by/4.0/).

increase its hydrophilicity, thereby facilitating cellular interactions [9–12]. This improves adhesion to the substrate and increases cellular stability. However, G overly hydrophobic surface makes it less suitable for cell adhesion. Further research and chemical modifications are required to improve its biocompatibility [13].

The interaction between GO and cells is greatly influenced by its physicochemical properties. GO surface, along with its mechanical and chemical properties, makes it a suitable material for tissue engineering scaffolds. These properties facilitate cell adhesion, proliferation and differentiation, all of which are essential for tissue regeneration. According to one study, GO was found to enhance cellular processes crucial for repairing and regenerating structures such as bones, skin, and nerves [14].

Reference [15] presents research on micro- and nanofibrous silk scaffolds containing GO and reduced GO (rGO). The results showed that Neuronoma NG108-15 cells adhered to and exhibited viability on all substrates, while increased proliferation and metabolic activity were observed on scaffolds containing GO additives compared to unmodified silk fibres. This trend increased linearly as the additive content increased. Research conducted by Convertino *et al*. showed that the length of PC12 cell neurites increased by 27% after five days of culture on substrates supplemented with GO, compared to cells cultured on standard substrates. The potential use of G to improve nerve impulse conduction was also highlighted; this phenomenon is attributed to the elongation of neurons, particularly their processes [16].

In their study, Park *et al*. analysed the differentiation of human neural stem cells (hNSCs) on culture slides containing a G film on unmodified substrates. After three days of observation, no significant differences in cell physiology were noted; however, after 21 days of culture, the differences were clearly noticeable. The area covered with G nanoparticles was uniformly populated by cells with very high confluence. In contrast, on the unmodified substrate, the cells were distributed unevenly, likely due to low adhesion. After another week of culture, the cells exhibited an elongated shape and significantly better growth on the G-coated culture glass. The number of neurons and glial cells at a given location was also determined, and the results showed that, in cultures using GO, the number of neurons was double the number of glial cells, which may indicate support for differentiation towards neurons. A key aspect of stem cell-based therapy is to induce hNSCs to differentiate into neurons rather than glial cells, the latter of which support neurons but do not replace their functions [6, 8].

Reference [17] presents the results of in vitro studies investigating the impact of G on primary rat cortical neurons. The neurons were cultured on a copper foil onto which G layers were deposited using the chemical vapour deposition (CVD) method. The next step was to transfer them to plastic polymer plates. The cultures were conducted on G-coated surfaces, while the control group consisted of unmodified plates and plates coated with a poly-D-lysine (PDL) polymer to promote neuronal attachment and growth. Cell viability analysis, cytotoxicity testing, and phase-contrast microscopy were performed. The researchers observed strong adhesion to the polymer substrate; however, the degree of neuronal adhesion to G was significantly higher than to the unmodified surface. The absence of G toxicity was also demonstrated, with significantly lower lactate dehydrogenase (LDH) levels observed than on uncoated substrates. Analysis using phase-contrast microscopy enabled neuronal attachment and the formation of long nerve processes to be visualised. These results indicate the normal metabolism and morphology of the studied structures.

Feng *et al*. published a study on the effect of matrices with varying GO and rGO contents on the biological functions of adipose derived stem cells (ADSCs). GO was shown to have a beneficial effect as a scaffold component in the case of neuronal differentiation of cells compared to the control [18].

Li *et al*. also described the potential use of G, as a substrate for neuronal growth. Compared to the control group, which was cultured on a commonly used polystyrene plate, they observed a significant increase in the number of neurites and their average length over a period of 2–7 days. G was found to most strongly support the proliferation and elongation of neurites, particularly on the second day of neuronal development. Western blot analysis showed that GO significantly supported the expression of the GAP-43 protein, an effective marker of growth cones, thus influencing the stimulation of neuronal proliferation and axon growth [19].

Numerous studies have investigated the potential application of G and GO in stem cell therapy, wound healing, regenerative medicine and tissue engineering, and the results indicate their high biocompatibility and broad potential applications in medicine [20–23]. However, few reports in the literature address the morphology, growth promotion, viability, and differentiation of microglia on G- and GO-coated substrates. This aspect is particularly important in modern regenerative medicine and may contribute to the development of therapies that support the recovery and full rehabilitation of neurological patients. The results of the studies conducted may also supplement current knowledge regarding the potential to promote the growth of HMC3 cells cultured on G and GO substrates.

2. Materials and methods

The study was conducted on three test groups:

- Si – 2-inch CZ-Si dummy silicon wafers with a thickness of 500 μm ± 50 μm, single-sided polished (ssp),
- SiG – silicon wafers measuring 10 × 10 mm, with G deposited by the CVD method, purchased from Graphenea,
- SiGO – CZ-Si dummy silicon wafers with a diameter of 2 inches and a thickness of 500 μm ± 50 μm, single-sided polished (ssp), serving as a substrate on which a dispersed aqueous suspension of GO with a concentration of 4.5 g/l, purchased from the Institute of Electronic Materials Technology (ITME), using the spin coating method. This method allows for the uniform distribution of the suspension on the surface due to a centrifugal force and removal of excess suspension (POLOS Spin150i-NPP, SPS-Europe B.V., Putten, The Netherlands) at a rotational speed of 2500 rpm. The deposition of GO on the tested surfaces was made possible by their prior activation and cleaning using 100 W RF plasma (Plasma Prep III, Westchester,

PA, USA). References [24–26] indicate that this procedure increases hydrophilicity, leading to a uniform and durable deposition of GO nanostructures on the surface. After depositing the GO layer, the samples were dried in a vacuum oven (Vacucell 22L) at 40 °C for 24 h.

3. Research results

3.1. Structural studies

The surfaces of unmodified silicon (Si) wafers and modified silicon (SiG, SiGO) wafers were imaged using an electron-multiplying charge-coupled device detector (EMCCD) coupled to a Quanta 250 field emission gun (FEG) scanning electron microscope (SEM) (FEI, Hillsboro, OR, USA). An accelerating voltage of 10 kV and a spot size of 3 were used. A minimum of 10 images were taken at random locations for each sample examined.

Fourier transform infrared spectroscopy (FTIR) using a Nicolet IS50 instrument (Thermo Fisher Scientific, Waltham, MA, USA) was used to identify carbon groups characteristic of the presence of GO (carbonyl, carboxyl, and hydroxyl). The wavelength range used was 4000-400 cm^{-1}, and the measuring device had a resolution of 4 cm^{-1}.

The surface topography and roughness of the samples were measured using a Zeiss LSM 700 confocal microscope equipped with a 405 nm laser and an optical resolution of approximately 300 nm.

3.2. THz radiation

To perform experiments in the THz range, the following samples were prepared: (1) a thin silicon layer (Si), (2) a G layer (SiG), and (3) a GO layer (SiGO), each mounted on a silicon substrate on a thicker silicon wafer.

Measurements were carried out using a TPS Spectra 3000 time-domain spectrometer (THz-TDS) (TeraView Ltd., Cambridge, UK). This system uses a photoconductive antenna emitter and detector, which are driven by a femtosecond laser operating at a central wavelength of around 800 nm.

The effective frequency range was 0.1–3 THz. Measurements were performed in specular reflection mode. Each measurement consisted of 1000 averages. All measurements were conducted under a dry-air purge to minimise water-vapour absorption.

3.3. Surface roughness testing

The surface roughness of the Si, SiG, and SiGO samples was analysed using a Mitutoyo SJ-201 device (Mitutoyo Corporation, Takatsu, Kawasaki, Japan). Measurements were taken five times at different locations on each sample. The Ra, Rz, and Rq parameters, as well as the arithmetic means and standard deviations, were determined.

3.4. Biological studies of the HMC3 cell line.

3.4.1. In vitro culture conditions for the HMC3 cell line

For the biological studies, a cell line derived from human embryonic brain tissue [HMC3, American Type Culture Collection (ATCC)] was used. This was cultured in Eagle's minimum essential medium (EMEM) (ATCC), supplemented with L-glutamine (ATCC 30-2003) and containing Earle's balanced salt solution, essential amino acids, 2 mM L-glutamine, 1 mM sodium pyruvate, and 1.5 g/L sodium bicarbonate. The culture was then incubated at 37 °C in an incubator (HERAcell VIOS 160i, Thermo Scientific, Waltham, MA, USA) under conditions of 95% humidity and in an atmosphere containing 5% CO_2.

The test samples in their as-received state (Si) and with a modified surface layer (SiG, SiGO) were sterilised by exposure to a 70% ethanol solution for approximately 15 min and UV-C radiation for 30 min. Sample fragments were placed in a multi-well plate and 1 ml of a cell suspension containing 10^4 cells/well was added to each well. The plate was then incubated for either 24 or 48 h at a temperature of 37 °C, with a CO_2 concentration of 5% and a humidity of 95% (HERAcell VIOS 160i, Thermo Scientific, Waltham, MA, USA).

3.4.2. Cell culture and viability assay

Human microglial cells HMG-3 (ATCC® CRL-3304™) were used as an in vitro model to evaluate the cytocompatibility of the investigated substrates. Cells were cultured under standard conditions in a humidified atmosphere at 37 °C with 5% CO_2 using a complete growth medium appropriate for microglial cells.

For viability experiments, HMG-3 cells were seeded at a density of 5×10^5 cells per sample onto crystalline silicon (Si) plates either uncoated or coated with G or GO, as well as onto standard tissue culture polystyrene plates used as the control. The tested surfaces included bare silicon (Si) plates, silicon plates coated with G, and silicon plates coated with GO (GO–Si). After seeding, cells were incubated for 24 h to allow adhesion and initial cell-material interactions.

Cell viability was assessed using the PrestoBlue™ cell viability reagent (Thermo Fisher Scientific, Waltham, MA, USA), according to the manufacturer's protocol. Briefly, after 24 h of incubation, the culture medium was replaced with fresh medium containing PrestoBlue reagent and incubated for 1 h under standard culture conditions. Fluorescence was measured using a microplate reader, and the obtained values were normalised to the control polystyrene surface, which was defined as 100% cell viability.

3.4.3. Morphology of HMC3 cell line

To improve conductivity SEM imaging quality, the cells were fixed with a mixture of 4% paraformaldehyde and 0.4% glutaraldehyde (both Sigma-Aldrich, Burlington, MA, USA). Next, the cells were stained in a 1% solution of osmium tetroxide (OsO_4) (Sigma-Aldrich, Burlington, MA, USA) at 4 °C and then dehydrated in a gradient of ethanol and acetone (both POCH, Gliwice, Poland) at concentrations ranging from 30% to 100%. The samples were then dried at the critical point using a Leica EM CPD300. To create a conductive layer, a layer of gold was sputtered onto the surface (3 nm thick) using a Leica EM ACE 200 sputtering system.

4. Research results

4.1. Structural studies

Figure 1 shows the results of the structural analysis of the surface of the as-received silicon (Si), obtained via SEM [Fig. 1(a)], confocal microscopy analysis [Fig. 1(b)], and topography analysis [Fig. 1(c)].

The same analyses were performed on samples coated with G (SiG) [Fig. 1(d) and (f)] and GO (SiGO) [Fig. 1(g) and (i)]. SEM was used to analyse the surface condition of Si wafers, revealing the presence of deposited nanostructures (Fig. 1). Localised structural defects were observed on the SiG surface [Fig. 1(b)]. The GO deposited on the samples formed a continuous layer. The boundaries of the GO flakes are visible as bright edges.

Analysis of the surface topography using a confocal microscope showed that the material exhibits a low roughness of 9–14 µm in its as-delivered state and with deposited G (Si, SiG) [Fig. 1(b), (d)], as is evident in the 3D profiles of the examined surfaces [Fig. 1(a) and (c)]. The material with deposited GO is rougher, with measured parameters reaching values of up to 80 µm. The 3D profile also indicates the granularity of the examined structure, showing that the deposition of GO causes surface development and an increase in roughness parameters.

4.2. Fourier-transform infrared spectroscopy (FTIR)

FTIR spectra were recorded within the 4000–400 cm^{-1} range. Characteristic absorption bands corresponding to the presence of G nanostructures were observed for the SiGO and SiG samples (Fig. 2). Absorption peaks at wavelengths of 3084–3130 cm^{-1} represent O–H stretching vibrations, while absorption maxima in the 2917–2918 cm^{-1} range correspond to aliphatic bonds. Analysis of the provided spectra revealed groups corresponding to the deformational vibrations of O–H bonds (1420–1432 cm^{-1}), and peaks in the 1000–1153 cm^{-1} range were found to be characteristic of stretching vibrations of C–O groups.

The absorption bands observed in the FTIR spectrum, corresponding to the vibrations of O–H and C–O groups, may be associated with the presence of organic residues remaining from the CVD G transfer process, particularly polymethylmethacrylate (PMMA) residues, as well as with partial oxidation of the G surface during the transfer and sample preparation processes. The intensity of these bands may also be related to the presence of oxygen-containing functional groups within the CVD G structure and to the adsorption of moisture and other oxygen-containing compounds from the surrounding environment. Therefore, the presence of the O–H and C–O bands in the analysed samples may be attributed to the G preparation and transfer

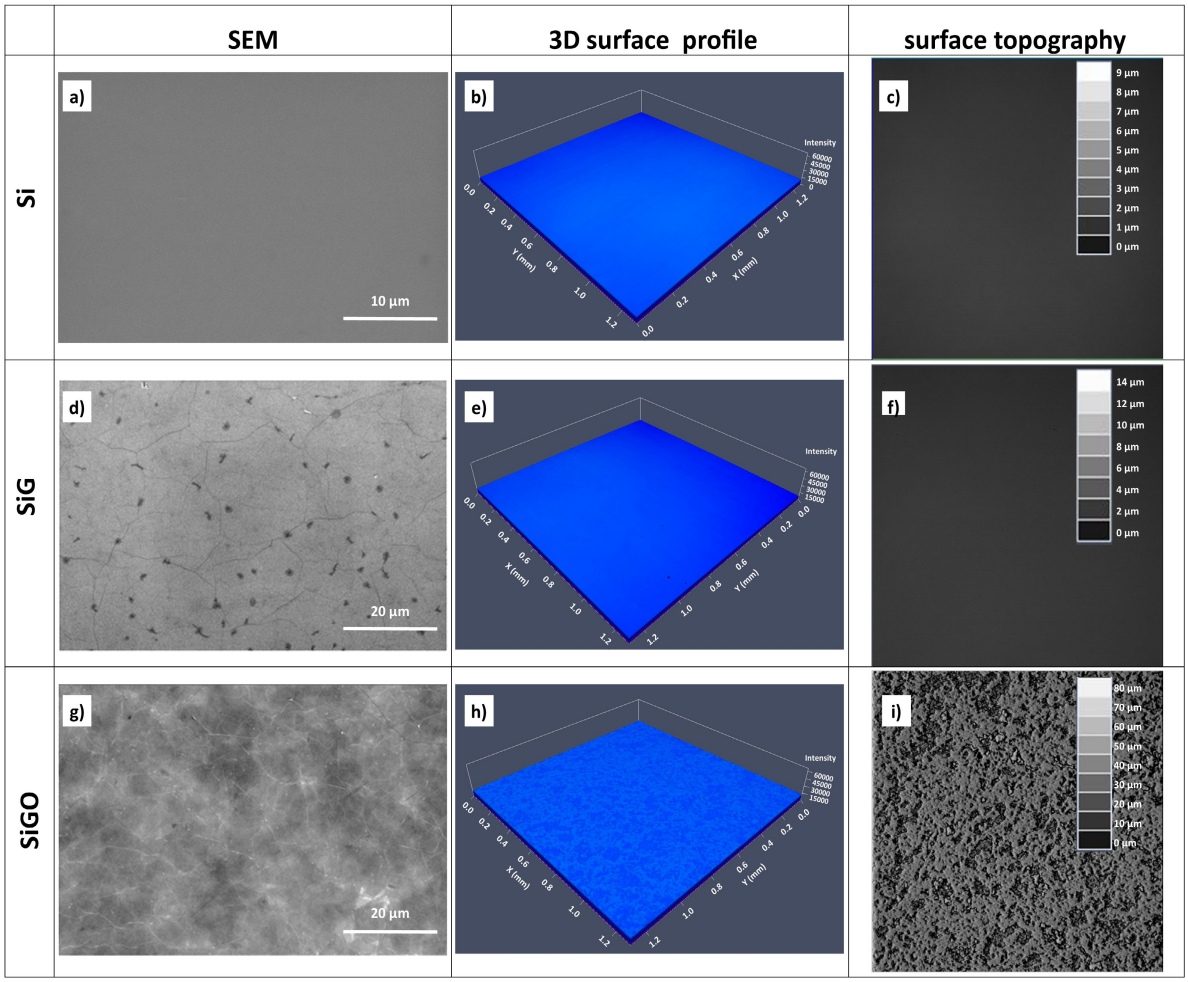


Fig. 1. Structural analysis of the surfaces of silicon wafers in their as-delivered state (Si), after deposition of G (SiG), and GO (SiGO), performed using a Quanta 250 FEG SEM for Si samples (a), SiG (d), SiGO (g), as well as Zeiss LSM 700 confocal microscopy for Si (b) and (c), SiG (e) and (f), and SiGO (h) and (i).

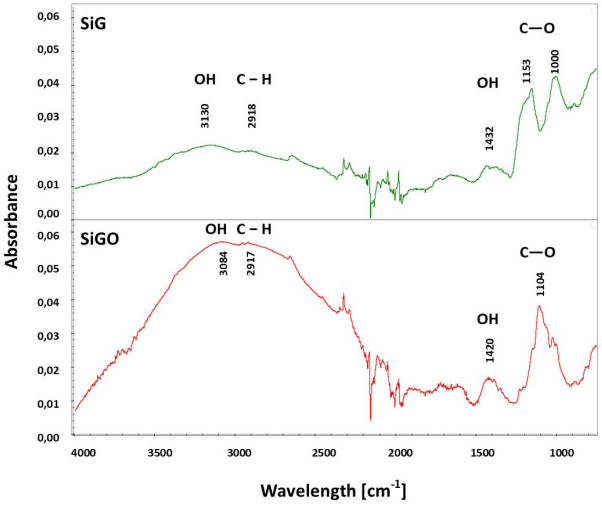


Fig. 2. FTIR spectra of SiG and SiGO samples.

processes, possible surface functionalisation of the material, as well as the adsorption of components from the surrounding environment.

4.3. *THz radiation*

Terahertz time-domain spectrometer (THz-TDS) measurements performed in reflection mode confirm the expected behaviour. The investigated samples are based mainly on silicon, whose refractive index in this frequency range is approximately 3.4, resulting in strong Fresnel reflections. Owing to the parallel interfaces of the substrate/wafer, multiple internal reflections occur and manifest as Fabry-Pérot oscillations in the time-domain signal. The time-domain THz waveforms are shown in Fig. 3(a) and (b). Since the signals are normalised, the amplitude of the first peak appears similar for all samples. However, due to its higher conductance, G reflects more incident THz radiation than GO. Consequently, less radiation is coupled into the SiG sample [Fig. 3(b)] than into the SiGO sample [Fig. 3(a)]. As a result, the second peak – corresponding to the first reflection from the backside of the wafer – is significantly smaller for SiG than for SiGO.

Additionally, the figures reveal a difference in the temporal position of the secondary pulse. For the SiGO sample, the secondary pulse occurs approximately 19 ps after the primary pulse, whereas for the SiG sample, it appears after approximately 20.5 ps. A propagation-time difference of $\Delta t = 1.5$ ps in silicon, with a refractive index of $n = 3.42$, corresponds to a wafer thickness difference of $\Delta d = c \cdot \Delta t / 2n = 65.8$ µm. This value lies within the thickness tolerances typically specified by silicon wafer suppliers and may additionally result from the fact that the SiG and SiGO samples were obtained from different vendors.

4.4. *Surface roughness*

Figure 4 shows a graph of surface roughness of the tested samples. The Ra, Rz, and Rq parameters, their arithmetic means, and standard deviations were determined. Analysis of the surface roughness measurement results shows that, for all examined parameters (Ra: arithmetic mean roughness; Rz: arithmetic mean of the five highest profile height

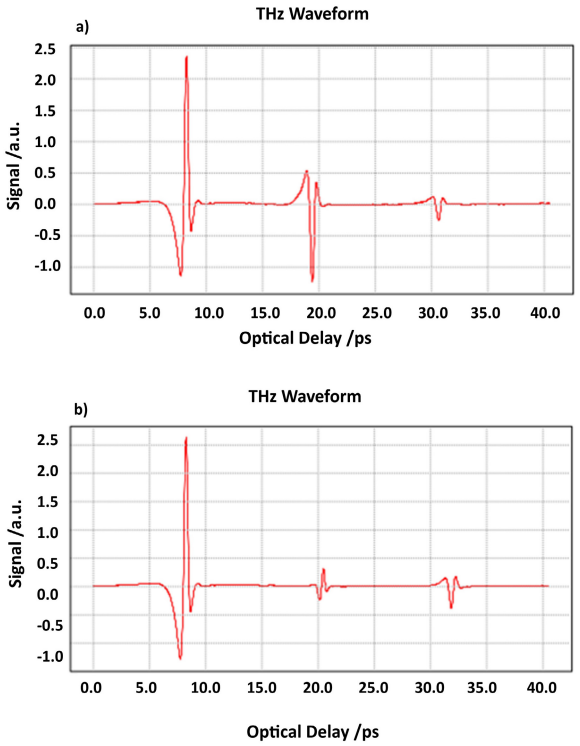


Fig. 3. Time trace of the THz pulse obtained for GO layer on silicon substrate (SiGO) (a) and G layer on silicon substrate (SiG) (b).

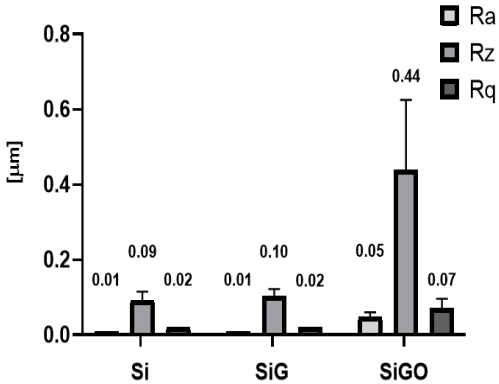


Fig. 4. This graph shows the surface roughness of the samples tested (Si, SiG, and SiGO).

values; Rq: root mean square profile deviation), the highest values were recorded for silicon surfaces with a deposited GO (SiGO) layer.

4.5. *Viability of HMC-3 human microglial cells cultured on silicon-based substrates*

Figure 5 shows a graph of the viability of HMC3 cells after a 24 h incubation period. The cells were seeded onto test samples of the material in its as-delivered state (Si), with either a layer of G (SiG) or GO (SiGO) deposited on the surface. This is shown relative to the control sample, which consists of a culture on a polystyrene plate. The percentage of viability was determined using the PrestoBlue assay.

An analysis of the HMC3 cell viability following contact with Si, SiGO, and SiG surfaces revealed the lowest percentage of viable cells – approximately 85% – when

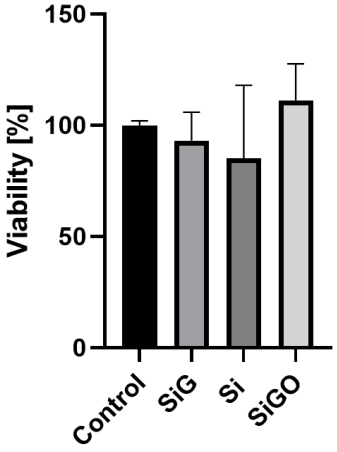


Fig. 5. This graph shows the cell viability of HMC3 cells seeded onto the surfaces of Si, SiG, and SiGO samples after 24 h of incubation, compared to the control sample (a culture on a polystyrene plate).

cultured on silicon wafers. A significant increase in a microglial cell survival was observed when they were grown on a substrate with a deposited layer of GO (111%). For the SiG substrate, the viability of the tested cells was lower than that observed in cultures on SiGO plates and compared to the control group; however, G proved to be more effective in stimulating cell growth than unmodified silicon material.

4.5.1. Morphology of HMC3 cells

Figure 6 shows the results of the surface morphology analysis of HMC3 cells seeded on silicon wafers. Figure 7(a) and (b) shows the results of the analysis of materials coated with G, and Figure 8(a) and (b) shows the results of the analysis of GO. All analyses were performed using a Quanta 250 FEG SEM, and structures marked with a red arrow are visible in all figures.

Analysis of images of silicon wafers on which microglial cells had been cultured (Fig. 6) revealed a uniform surface, enabling cell adhesion and structure to be observed. The cells were evenly distributed across the entire surface of the sample and numerous projections forming a network of connections between the cells were visible. Regarding the morphology of the cells seeded onto a material with a deposited G layer (SiG) [Fig. 7(a) and (b)], a uniform distribution was observed. However, despite their well-developed processes, the cells exhibited significantly lower proliferation. The cells were characterised by a smaller number of cellular branches with a reduced length compared to cultures on SiGO substrates.

The surface structure of SiG is homogeneous, but G flakes can be seen peeling off in many places. The highest level of cell proliferation was observed on a substrate with a deposited layer of GO (SiGO) [(Fig. 8(a) and (b)]. A high number of long cellular processes were observed, forming a complex network of connections, as can be seen particularly clearly in Fig. 8(a) and (b). The cells were evenly distributed across the analysed surface and exhibited greater variation in shape. Flattening of the cells was also observed, indicating good adhesion to the substrate. The microglial structures showed no signs of shrinkage or deformation. Fewer detached

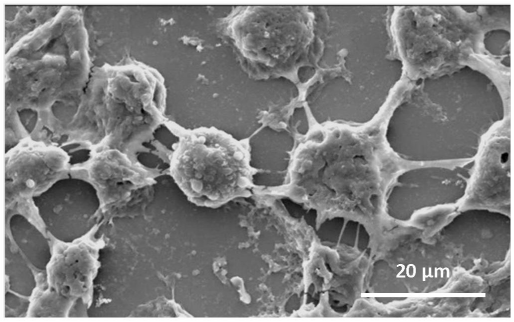


Fig. 6. This image shows the morphology of HMC3 cells seeded on a silicon substrate, as captured using a Quanta 250 FEG SEM.

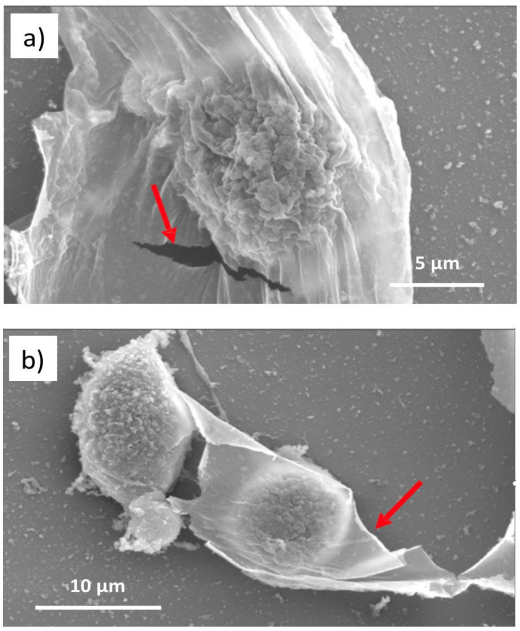


Fig. 7. The morphology of HMC3 cells seeded on a silicon substrate coated with a layer of G was imaged using a Quanta 250 FEG SEM (a) and (b).

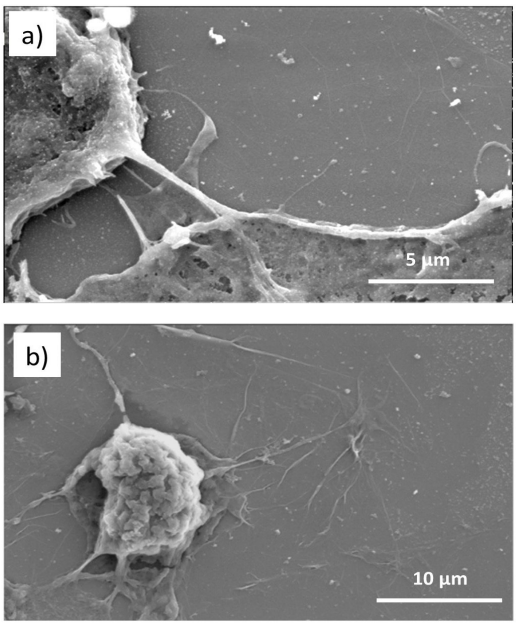


Fig. 8. The morphology of HMC3 cells seeded on a silicon substrate coated with a layer of GO was imaged using a Quanta 250 FEG SEM (a) and (b).

G flakes were also observed, indicating a more uniform surface than that of the SiG substrate. GO successfully supports the multiplication, growth and proliferation of HMC3 cells.

5. Discussion

Using confocal microscopy techniques, topographical characteristics of the examined surfaces and 3D profiles were obtained. The results of the analysis indicate the highest surface roughness in samples with a deposited GO layer, which is consistent with the roughness measurements. In the case of samples in their as-delivered Si state, the surface under examination is flat, whereas structural defects are noticeable in materials with deposited G.

Analysis of the surface condition using scanning electron microscopy of modified silicon wafers and FTIR spectroscopy confirmed the presence of deposited structures; distinct boundaries of G flakes were observed, as well as particularly in the case of SiG samples, the phenomenon of G sheet delamination. FTIR studies confirmed the presence of G and GO nanoparticles, including characteristic peaks corresponding to hydroxyl and carbonyl groups, as well as aliphatic bonds.

In studies of degree of interaction between THz radiation and a silicon substrate on which GO (SiGO) and G (SiG) were deposited, it was observed that G reflects more of the radiation incident on the sample than GO, which results from G higher conductivity. For all tested samples, multiple internal reflections within the materials were observed.

Surface roughness measurements revealed the greatest increase in Ra, Rz, and Rq parameters when the silicon surface layer was modified with GO (SiGO). The surface roughness values of the purchased materials (Si and SiG) were comparable.

Analysis using the PrestoBlue assay on HMC3 microglial cells showed that GO most effectively stimulated their viability. The G substrate provided better conditions than the silicon material in its as-delivered state; however, the viability of cells seeded on this sample turned out to be lower than in the control sample, i.e., the culture on a polystyrene plate. Referring to the results of surface roughness measurements and topography analysis, it can be concluded that the surface with a deposited layer of GO (SiGO) was the most developed, and microglial cells adhered more readily to this material. The influence of various surface properties, including roughness, on cell behaviour has been extensively described in [27, 28]. It can therefore be concluded that HMC3 microglia also exhibit better proliferation, viability, and adhesion when cultured on developed surfaces.

Analysis of the morphology of HMC3 cells showed that on silicon substrates, the cells were evenly distributed with high adhesion; numerous, well-developed processes were observed, but their proliferation was significantly lower compared to cultures on other substrates. When SiGO was used, the cells had significantly longer, highly branched processes and exhibited high metabolic activity. For SiG samples on which HMC3 cells were seeded, uniform dispersion of the cells across the tested surface was observed; however, they exhibited much lower proliferation, and their number and length were reduced.

The conducted studies and their analysis indicate that GO effectively stimulates the growth and proliferation of HMC3 microglial cells. Modifying the silicon surface by depositing a layer of GO promoted cell adhesion. G nanoparticles, on the other hand, created poorer conditions for the growth of the tested cells; their biological activity was lower than in cultures on an unmodified silicon surface or a polystyrene plate.

The potential application of GO in regenerative medicine as a basis for developing new techniques or platforms for nerve cell culture requires further research. However, it represents an innovative solution that could contribute to the development of more effective biomaterials for nerve regeneration than those currently available and address challenges associated with culturing microglial cells in vitro.

6. Conclusions

An analysis of the research results led to the following conclusions:

- Deposition of G did not cause a significant increase in surface roughness compared to GO. The latter caused the Ra, Rz, and Rq roughness parameters to increase by 400%, 340%, and 250%, respectively, compared to a silicon wafer.
- G reflected more incident THz radiation than GO.
- Increase in the viability of HMC3 cells was observed on materials coated with GO after a 24 h incubation period (an 11% increase compared to the control group).
- Culture on a SiGO substrate was found to be the most effective in supporting normal cell growth, adhesion, and proliferation.

The research results presented here indicate the effectiveness of GO in supporting the viability and proliferation of human microglial cells, a result of changes in surface morphology. The effectiveness of the GO deposition methodology was confirmed, and it was demonstrated that less THz radiation interacts with the SiGO material. Consequently, silicon material with a GO layer may be an effective solution for developing biosensors and regenerative medicine scaffolds for cell growth.

References

[1] Liu, X. *et al*. Functionalized carbon nanotube and graphene oxide embedded electrically conductive hydrogel synergistically stimulates nerve cell differentiation. *ACS Appl. Mater. Interfaces* **9**, 14677–14690 (2017). https://doi.org/10.1021/acsami.7b02072

[2] Pabari, A., Yang, S. Y., Seifalian, A. M. & Mosahebi, A. Modern surgical management of peripheral nerve gap. *J. Plast. Reconstr. Aesthet. Surg.* **63**, 1941–1948 (2010). https://doi.org/10.1016/j.bjps.2009.12.010

[3] Reddy, S. *et al*. Allotropic carbon (graphene oxide and reduced graphene oxide) based biomaterials for neural regeneration. *Curr. Opin. Biomed. Eng.* **6**, 120–129 (2018). https://doi.org/10.1016/j.cobme.2018.05.001

[4] Fabbri, R. *et al*. Graphene glial-interfaces: Challenges and perspectives. *Nanoscale* **13**, 4390–4407 (2021). https://doi.org/10.1039/D0NR07824G

[5] Banker, G. & Goslin, K. *Culturing Nerve Cells, 2nd edition*. (MIT Press, 1998).

[6] Park, S. *et al*. Enhanced differentiation of human neural stem cells into neurons on graphene. *Adv Mater.* **23**, H263–H267 (2011). https://doi.org/10.1002/adma.201101503

[7] Zhang, Y. *et al*. Cytotoxicity effects of graphene and single-wall carbon nanotubes in neural phaeochromocytoma-derived PC12 cells. *ACS nano* **4**, 3181–3186 (2010). https://doi.org/10.1021/nn1007176

[8] Ryu, S. & Kim, B.-S. Culture of neural cells and stem cells on graphene. *Tissue Eng. Regen. Med.* **10**, 39–46 (2013). https://doi.org/10.1007/s13770-013-0384-6

[9] Hu, X., Yu, Y., Hou, W., Zhou, J. & Song, L. Effects of particle size and pH value on the hydrophilicity of graphene oxide. *Appl. Surf. Sci.* **273**, 118–121 (2013). https://doi.org/10.1016/j.apsusc.2013.01.201

[10] Lee, W. C. *et al*. Origin of enhanced stem cell growth and differentiation on graphene and graphene oxide. *ACS Nano* **5**, 7334–7341 (2011). https://doi.org/10.1021/nn202190c

[11] Aryaei, A., Jayatissa, A. H. & Jayasuriya, A. C. The effect of graphene substrate on osteoblast cell adhesion and proliferation. *J. Biomed. Mater. Res.* **102**, 3282–3290 (2014). https://doi.org/10.1002/jbm.a.34993

[12] Kim, J. *et al*. Bioactive effects of graphene oxide cell culture substratum on structure and function of human adipose-derived stem cells. *J. Biomed. Mater. Res.* **101**, 3520–3530 (2013). https://doi.org/10.1002/jbm.a.34659

[13] Morotomi-Yano, K., Hayami, S. & Yano, K. Adhesion states greatly affect cellular susceptibility to graphene oxide: Therapeutic implications for cancer metastasis. *Int. J. Mol. Sci.* **25**, 1927 (2024). https://doi.org/10.3390/ijms25031927

[14] Zare, P., Aleemardani, M., Seifalian, A., Bagher, Z. & Seifalian, A. M. Graphene oxide: Opportunities and challenges in biomedicine. *Nanomaterials* **11**, 1083 (2021). https://doi.org/10.3390/nano11051083

[15] Magaz, A., Li, X., Gough, J. E. & Blaker, J. J. Graphene oxide and electroactive reduced graphene oxide-based composite fibrous scaffolds for engineering excitable nerve tissue. *Mater. Sci. Eng. C* **119**, 111632 (2021). https://doi.org/10.1016/j.msec.2020.111632

[16] Convertino, D., Luin, S., Marchetti, L. & Coletti, C. Peripheral neuron survival and outgrowth on graphene. *Front. Neurosci.* **12**, 1 (2018). https://doi.org/10.3389/fnins.2018.00001

[17] Sahni, D. *et al*. Biocompatibility of pristine graphene for neuronal interface. *J. Neurosurg. Pediatr.* **11**, 575–583 (2013). https://doi.org/10.3171/2013.1.PEDS12374

[18] Feng, Z.-Q. *et al*. Neurogenic differentiation of adipose derived stem cells on graphene-based mat. *Mater. Sci. Eng. C* **90**, 685–692 (2018). https://doi.org/10.1016/j.msec.2018.05.019

[19] Li, N. *et al*. The promotion of neurite sprouting and outgrowth of mouse hippocampal cells in culture by graphene substrates. *Biomaterials* **32**, 9374–9382 (2011). https://doi.org/10.1016/j.biomaterials.2011.08.065

[20] Chen, G.-Y., Pang, D.W.-P, Hwang, S.-M., Tuan, H.-Y. & Hu, Y.-C. A graphene-based platform for induced pluripotent stem cells culture and differentiation. *Biomaterials* **33**, 418–427 (2012). https://doi.org/10.1016/j.biomaterials.2011.09.071

[21] Nolan, K., Millet, Y., Ricordi, C. & Stabler, C. L. Article commentary: Tissue engineering and biomaterials in regenerative medicine. *Cell Transplant.* **17**, 241–243 (2008). https://doi.org/10.3727/096368908784153931

[22] Lee, W. C. *et al*. Origin of enhanced stem cell growth and differentiation on graphene and graphene oxide. *ACS Nano* **5**, 7334–7341 (2011). https://doi.org/10.1021/nn202190c

[23] Lu, B. *et al*. Graphene-based composite materials beneficial to wound healing. *Nanoscale* **4**, 2978–2982 (2012). https://doi.org/10.1039/c2nr11958g

[24] Nasiłowska, B., Skrzeczanowski, W., Bombalska, A. & Bogdanowicz, Z. Laser emission spectroscopy of graphene oxide deposited on 316 steel and Ti6Al4V titanium alloy suitable for orthopedics. *Materials* **16**, 2574 (2023). https://doi.org/10.3390/ma16072574

[25] Kalela, N., Darpe, A. & Bijwe, J. Low pressure plasma induced surface changes of some stainless steels. *Surf. Coat. Technol.* **425**, 127700 (2021). https://doi.org/10.1016/j.surfcoat.2021.127700

[26] Sönmez, T., Fazeli Jadidi, M., Kazmanli, K., Birer, Ö. & Ürgen, M. Role of different plasma gases on the surface chemistry and wettability of RF plasma treated stainless steel. *Vacuum* **129**, 63–73 (2016). https://doi.org/10.1016/j.vacuum.2016.04.014

[27] Michaels, C., Keller, J., Stanford, C. & Solursh, M. In vitro cell attachment of osteoblast-like cells to titanium. *J. Dent. Res.* **68**, 276–281 (1989).

[28] Bowers, K. T., Keller, J. C., Randolph, B. A., Wick, D. G. & Michaels, C. M. Optimization of surface micromorphology for enhanced osteoblast responses in vitro. *Int. J. Oral. Maxillofac. Implants* **7**, 302–310 (1992).